Current Biology 19, 1861–1868, November 17, 2009 ©2009 Elsevier Ltd All rights reserved DOI 10.1016/j.cub.2009.09.063

Report

The Fission Yeast TACC Protein Mia1p Stabilizes Microtubule Arrays by Length-Independent Crosslinking

Rahul Thadani,[1,2] Yuen Chyao Ling,[1,2] and Snezhana Oliferenko[1,*]
[1]Temasek Life Sciences Laboratory, 1 Research Link, Singapore 117604, Singapore

Summary

Microtubule (MT) arrays are mechanistic effectors of polarity specification and cell division. Linear bundles in which MTs are bridged laterally [1, 2] are dynamically assembled in systems ranging from differentiated metazoan cells to fungi in a process that remains poorly understood. Often, bundled MTs slide with respect to each other via molecular motors [3, 4]. In interphase cells of the fission yeast *Schizosaccharomyces pombe*, MT nucleation frequently occurs at preexisting arrays [5, 6]. As the nascent MT lengthens, stable antiparallel MT overlaps are thought to form through competition between motion of the minus-end-directed kinesin Klp2p [4] and braking force exerted by the accumulating lateral crosslinker Ase1p [7–9]. Here we show that Mia1p/Alp7p, a transforming acidic coiled-coil (TACC) protein [10, 11], functions as a length-independent MT crosslinker. In cells lacking Mia1p MT-bundling activity, linear arrays frequently disassemble, accompanied by a marked increase in Ase1p off rate and erratic motion of sliding MTs. We propose that the combined action of lateral length-dependent (Ase1p) and terminal length-independent (Mia1p) crosslinkers is crucial for robust assembly and stability of linear MT arrays. Such use of qualitatively distinct crosslinking mechanisms in tandem may point to a general design principle in the engineering of stable cytoskeletal assemblies.

Results and Discussion

In interphase cells, Mia1p-3GFP localized as dots along mCherry-α-tubulin-labeled microtubules (MTs) and was enriched at MT overlaps but also seen at MT plus ends (Figure 1A). Notably, Mia1p-3GFP fluorescence intensity peaked at edges of MT overlaps (Figures 1B and 1C) and only weakly correlated with overlap length ($r = 0.38$, $p < 0.01$, $n = 56$; see Figure S1A available online). Consistent with enrichment at MT minus ends, Mia1p partially colocalized with the γ-tubulin accessory factor Mto1p-mCherry (Figure 1D). We confirmed the MT plus-end localization of Mia1p by coimaging Mia1p-3GFP and the plus-end marker Tip1p-mCherry (Figure 1E).

Purified recombinant MBP-Mia1p (Figure S1B) cosedimented with taxol-stabilized MTs (Figure 1F) with a dissociation constant K_D of 0.88 μM (Figure 1G; Figure S1C). MBP-Mia1p also directly interacted with tubulin heterodimers (Figure S1D). When mixed with rhodamine-labeled MTs, purified tag-free Mia1p induced rapid appearance of MT bundles (Figure 1H). Transmission electron microscopy showed MTs tightly aligned in regions of linear bundling, leading to frequent appearance of fan-shaped structures (Figure 1I). We examined the orientation of MTs in bundles with polarity-marked MTs and found that 68% of bundles were antiparallel, whereas the remaining 32% were parallel (Figure 1J, $n = 59$ bundles). Recombinant His_6-Mia1p-GFP localized to MT overlaps when mixed with rhodamine-labeled MTs (Figures 1K and 1L). We thus concluded that in vitro, Mia1p promiscuously binds MTs to induce formation of linear bundles.

We then employed deletion mutagenesis to generate an Mia1p mutant specifically deficient in MT bundling. Based on a multiple alignment of transforming acidic coiled-coil (TACC) proteins, we detected three conservation peaks at amino acids 151–300, 301–387, and 388–474 of Mia1p (Figure S2A), indicating the boundaries of putative functional domains. Secondary structure prediction algorithms suggested that the region downstream of residue 150 was rich in α helices and contained coiled coils ([12], Figures S2A and S2B).

Ectopically expressed N-terminal (Mia1p-1-300-GFP) and C-terminal (Mia1p-301-474-GFP) deletion mutants of Mia1p both showed aberrant distribution compared to full-length Mia1p, which localized to MTs and the spindle pole bodies (SPBs) in wild-type (Figure 2A) and *mia1*Δ (Figure S3A) cells. Because Mia1p-1-300-GFP does not contain a nuclear export sequence [13], it was restricted to the nucleus, where it localized to spindle MTs (Figure 2A). However, this construct could bind cytoplasmic MTs when we disrupted the nuclear envelope with a temperature-sensitive RanGEF mutation [14] (Figure S3B). This suggested that Mia1p-1-300-GFP contained the de facto MT-binding activity. Conversely, Mia1p-301-474-GFP localized mainly to the SPBs and very weakly as dots on MTs but was depleted from MT overlaps (Figure 2A; Figure S3A). MBP-Mia1p-1-300 cosedimented with MTs in a spin-down assay, whereas MBP-Mia1p-301-474 did not (Figure 2B). Within the first 300 amino acids lies a conserved α-helical region spanning amino acids 151–300 (predicted to form a coiled coil at residues 244–256). A mutant protein lacking this region, MBP-Mia1p-Δ151-300, retained the ability to bind to MTs (Figure 2B). Strikingly, Mia1p-Δ151-300 failed to bundle MTs in vitro, unlike Mia1p and Mia1p-1-300 (Figure 2C). We concluded that MT-binding activity centered on Mia1p-1-300 and that the α-helical-rich region spanning residues 151–300 was crucial for MT bundling. The GFP-tagged bundling mutant Mia1p-Δ151-300-GFP, expressed under the native promoter, was abundant (Figure S3C) and localized to the SPB but was depleted from MTs (Figure 2D).

Our results thus far suggested that Mia1p might function as an MT crosslinker. Therefore, we examined interphase MT dynamics in *mia1Δ151-300* cells, where Mia1p could not bundle MTs. We observed comparable MT growth (2 ± 0.2 μm min^{-1} versus 2.3 ± 0.3 μm min^{-1}) and depolymerization (7.4 ± 0.02 μm min^{-1} versus 7.1 ± 0.02 μm min^{-1}) rates in wild-type and *mia1Δ151-300* cells. Both strains exhibited similar numbers of MT plus ends, labeled by an EB1 protein, Mal3p-GFP (11 ± 2 versus 12 ± 1.8, $n = 20$ cells), and comparable probabilities of survival of newly nucleated MTs (0.91, $n = 185$ MTs versus 0.84, $n = 200$ MTs). Concordantly, interaction of the MT-stabilizing protein Alp14p [15] with Mia1p (Figures S3D and S3E) and Klp2p recruitment to MTs (Figure S3F)

*Correspondence: snejana@tll.org.sg
[2]These authors contributed equally to this work

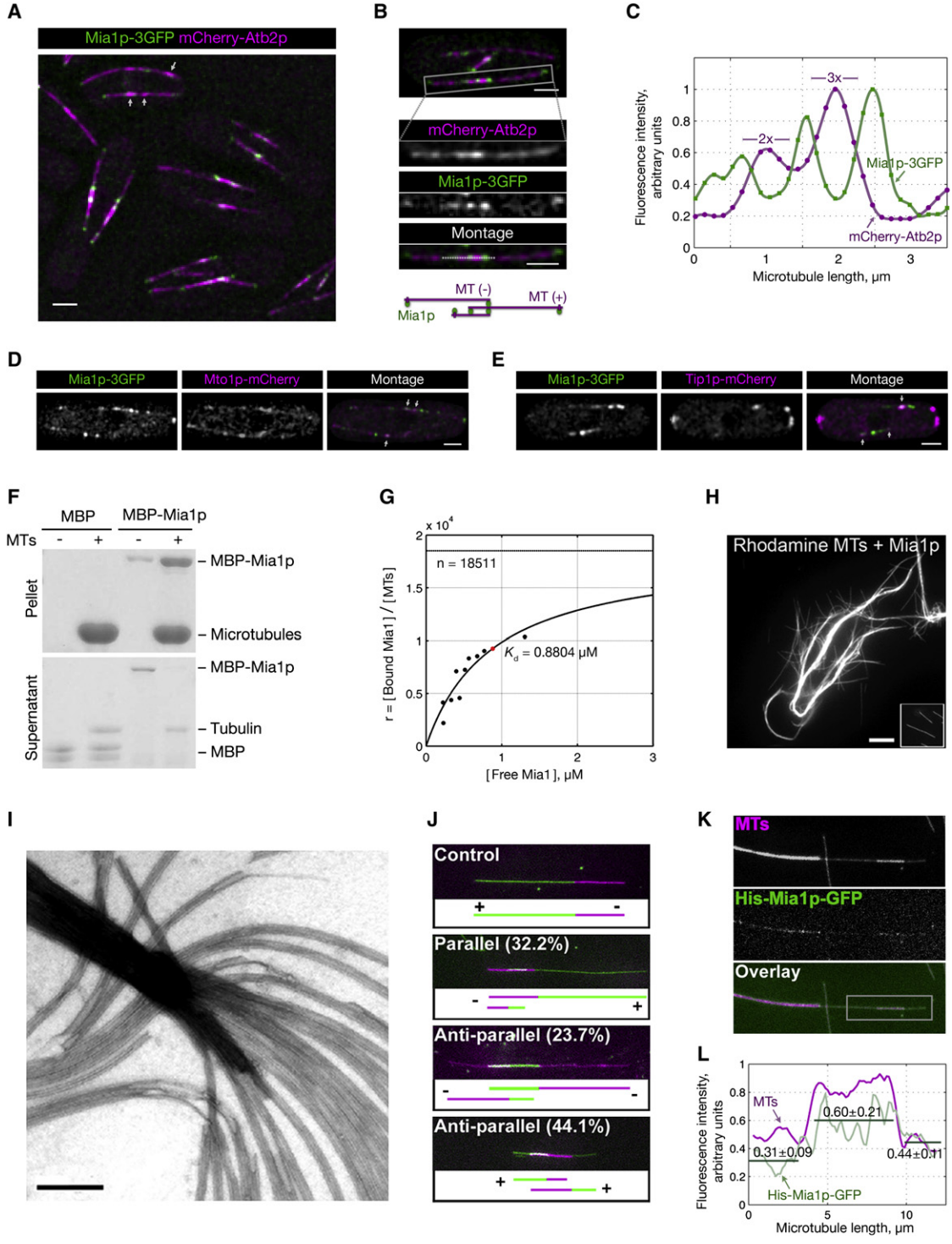

Figure 1. Mia1p Flanks Microtubule Overlaps In Vivo and Bundles Microtubules In Vitro

(A) Mia1p-3GFP (green) localizes along mCherry-α-tubulin-labeled microtubules (MTs) (magenta). Arrows mark a medial region of overlap and a nascent bundle at the periphery. Shown is a deconvolved maximum-intensity reconstruction. Scale bar represents 2 μm.

(B) Mia1p-3GFP flanks a medial MT overlap. Magnified: single confocal plane with a schematic interpretation (bottom). Scale bar represents 2 μm.

(C) Fluorescence intensity profiles of Mia1p-3GFP and mCherry-Atb2p along the dotted line shown in (B).

(D and E) Mia1p-3GFP partially colocalizes with Mto1p-mCherry (D) and Tip1p-mCherry (E). Shown is a maximum-intensity reconstruction of three confocal planes. Scale bar represents 2 μm.

(F) MBP-Mia1p copellets with taxol-stabilized MTs. MBP and MBP-Mia1p were incubated in the absence (−) or presence (+) of MTs and centrifuged through a glycerol cushion. Pellet and supernatant were separated by SDS-PAGE and stained with Coomassie blue.

(G) Dissociation constant K_D of the MBP-Mia1 complex with MTs, as determined by MT spin-down assays. Nonlinear regression was performed on the standard binding equation for a macromolecule containing n equivalent noninteracting ligand-binding sites.